Exploring the Inhibition of Cytochrome P450 2B6 by Phenobarbital through Computational Studies

Shankar.SM [1], David Stephen.A[1*], C. Natarajan[2] and Selvakumar.M [3]

[1] *Department of Physics, Hindusthan Institute of Technology, Coimbatore 641028, Tamilnadu, India*

[2] *The Principal, Hindusthan Institute of Technology, Coimbatore 641028, Tamilnadu, India*

[3] *Department of Science and Humanities, Sri Krishna college of Engineering and Technology, Coimbatore 641008, Tamilnadu, India*

*[1]*Corresponding author: davidstephen_dav@yahoo.co.in*

Abstract

*The inhibition activity of the historical antiepileptic drug phenobarbital (PB) on human cytochrome P450 2B6 (CYP2B6) has been investigated by computational methods. Both hydrophobic and electrostatic intermolecular interactions have been observed in docking analysis. The density functional calculations on gas phase inhibitor and the molecule lifted from the active site using 6-311G** basis set with the Gaussian09 program package showed almost negligible variation in geometrical parameters. The deformation density, Laplacian of electron density, atomic charges and electrostatic potential map of PB molecule in the active site are in agreement with the interaction between the ligand and the protein. The significantly higher dipole moment of PB in the active site compared to the gas phase provides additional evidence for strong inhibition of CYP2B6 by phenobarbital.*

Key words: *Phenobarbital, Cytochrome P450 2B6, Molecular docking, Topology, Atomic charges, Electrostatic potential*

1. Introduction

Epilepsy is a brain disorder causing seizures or unusual sensations and often loss of consciousness, affecting around 50 million people worldwide [1]. Although there are many antiseizure drugs available in the market, phenobarbital (Figure 1) is the most commonly prescribed drug to treat epilepsy for over a century ever since Alfred Hauptmann, serendipitously

discovered the anticonvulsant properties of this hypnotic drug[2]. Phenobarbital is a non-selective central nervous system (CNS) depressant that could act on γ-aminobutyric acid subtype receptors increasing synaptic inhibition. It affects the polysynaptic midbrain reticular formation and thus checks the CNS stimulation. Phenobarbital also inhibits glutamate induced depolarizations causing an elevation in seizure threshold and decline in the spread of seizure activity from a seizure center.

Many of the chemical reactions in drug metabolism are catalyzed by Cytochrome P450 proteins (CYP). This monooxygenase system consists of phospholipids, NADPH-cytochrome P450 reductase, cytochrome $b5$, and a multiplicity of CYP isoforms. Expressed primarily in the liver, cytochrome P450 2B6, a member of the cytochrome P450 family of enzymes, contributes 1%–11% to the total microsomal P450 pool [3]–[6]. Drugs of different classes like antiretrovirals, antifungals and antidepressants have been shown to inhibit CYP2B6 *in vitro*. Human CYP2B6 is inducible by rifampicin, phenytoin and Phenobarbital [7]–[9], of which induction by phenobarbital is the typical example of enzyme induction [10]. In cultured human hepatocytes, phenobarbital can lead to a 5- to 10-fold induction in enzyme protein levels as well as their activity[6], [8]. The analgesic drug metamizole, its metabolite AA, and antipyrine have been shown to induce human CYP2B6[11]. J. G. Zhang et al evaluated the concentration- and time-course induction of CYP2B6 by phenobarbital in detail. Lee et al have reported the effect of phenobarbital treatment on CYP2B6 expression in liver and brain and induction of *in vivo* nicotine disposition using African Green (Vervet) monkeys. Lovorco et al predicted the CYP2D6 binding affinity of a few substituted thioureas by means of iterative linear interaction energy approach, which served as a powerful model to develop ligand-binding affinity prediction tools. Recently, the induction potency of CYP2B6 by bupropion and efavirenz has been assessed in vitro and from clinical studies[12]. Though there are many *in vitro* and *in vivo* studies involving CYP2B6 enzyme and drug molecules, theoretical studies on the interaction of phenobarbital with CYP2B6 are sparsely found in the literature. Thus, in order to gain an insight, the binding of phenobarbital with human CYP2B6 enzyme has been studied using molecular docking after optimizing the structure of phenobarbital.

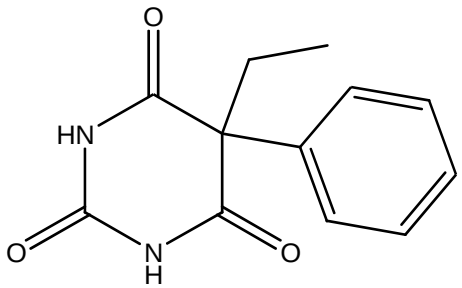

Figure 1. The chemical structure of phenobarbital

2. Computational details

The 3D-structure of human CYP2B6 (5UFG) was obtained from the Brookhaven Protein Data Bank. The ligand-protein intermolecular interactions were studied by Auto Dock 4.2 program[13] that generated 10 different conformations of the ligand. Discovery Studio 2017R2 software was used to view the PB-CYP2B6 complex. Table1 shows the binding energies of all the conformers with CYP2B6. Among all the conformers, conformer 1 pose the largest binding affinity (-3.61 kcal/mol) towards CYP2B6. In the gas phase calculations, the molecule was optimized with using DFT (B3LYP; 6-311G** basis set)[14], [15], while for the molecule lifted from the active site, a single point energy calculation was carried out. The electron density and Laplacian of electron density were determined from the Bader's theory of atoms in molecules (AIM)[16], [17] using *ext94b* routine with the help of AIMPAC software[18], [19]. The deformation and Laplacian of electron densities were plotted by *wfn2plots* and [20], [21]. Moliso[22] program suite was used to plot the electrostatic potential map.

3. Results and Discussion

3.1. Molecular docking and phenobarbital – cytochrome P450 2B6 interaction

Molecular docking, the process of searching a ligand that is energetically and geometrically able to fit in the active site of a protein, is being widely used to discover novel drugs. In the present study, the optimized molecular structure of phenobarbital was used for the molecular docking in the active site of cytochrome P450 2B6. Molecular docking was carried out to understand the binding affinity, molecular conformation and the orientation of phenobarbital molecule in the active site of cytochrome P450 2B6. The conformer with the lowest docking score value of -3.61 kcal/mol and binding affinity constant of 2.26μM (Table 1) was chosen and its interactions with the neighboring amino acids in the active site of cytochrome P450 2B6 was studied. Close

examination revealed hydrogen bonding (with the anionic sub-site and acyl binding site), hydrophobic and electrostatic interaction between phenobarbital and the binding site residues. In the acyl binding site, the C(18) atom of phenobarbital forms hydrogen bonding interaction with the nearby amino acid ARG253 at a distance of 4.14 Å, whereas the aromatic ring shows a Pi-acyl interaction with ARG253 at a distance of 4.73 Å (Table 2). Notably, in the hydrogen bonding, H(5) atom strongly interacts with GLU254 at a distance of 1.9 Å. The same atom also exhibits electrostatic Pi-cation interaction with HIS285 residue at a distance of 4.95 Å. Furthermore, in this site, O(1)...O (amino acid GLU250) interaction with distances of 2.49 Å was observed (Table 2). The 2D plot (Figure 2) shows the hydrogen bonding, hydrophobic and electrostatic interactions of phenobarbital in the active site of cytochrome P450 2B6.

Table 1. The lowest binding energies (kcal/mol) and inhibition constant (μM) of 10 different conformers of compounds.

S.NO	BE (Kcal/mol)	IC (μm)
1	-3.61	2.26
2	-3.59	3.48
3	-3.59	3.86
4	-3.54	4.20
5	-3.35	12.53
6	-3.35	3.50
7	-3.33	2.54
8	-3.29	2.33
9	-3.24	2.35
10	-2.59	3.60

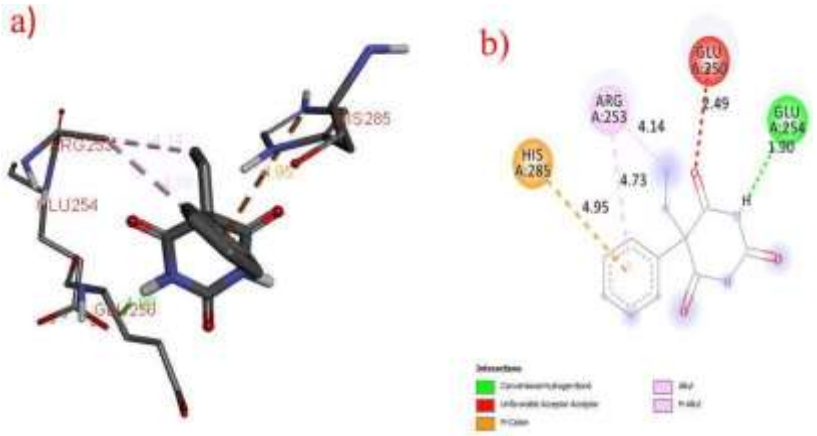

Figure 2. (a)-(b) Images showing the phenobarbital- cytochrome P450 2B6 complex and intermolecular interactions obtained by Biovia Discovery Studio 2017R2.

Table 2. Nearest neighbors and short contact distances (Å) of phenobarbital with amino acid residues of cytochrome P450 2B6 active site

Interacting species	Type	Distance(Å)
H(5)…GLU254/OE2	Conventional H-bond	1.9
O(1)…GLU250/O	Acceptor	2.49
C(18)…ARG253/CB	Alkyl	4.14
aromatic ring···ARG253/CB	Pi- Alkyl	4.73
aromatic ring···HIS285/NE2	Pi- Cation	4.95

3.2. Structural aspects

The optimized structure of phenobarbital is depicted as ball and stick model in Figure 3. The pertinent bond distances and bond angles are presented in Table 3. The geometrical parameters of both the gas phase molecule and the one lifted from the active site were found to be one and the same. Hence, one set of values are reported and discussed here. The structural overlay of PB molecule in gas phase and in active site region is shown in Fig.4. The three ring C=O bonds have a bond length of ~1.201 Å. The bond length of each N-H bonds is 1.021 Å. The bond lengths of all the C-N bonds in the pyrimidine ring are around 1.38 Å. The pyrimidine ring and the aromatic ring are bridged by C10-C11 bond, whose distance is 1.558 Å. To the same C10 carbon, an ethyl group is attached. The distance between the methylene carbon (C13) and C10 is found to be 1.552 Å. In the ethyl group, the bond length of C13-C18 is 1.531 Å. All the C-C bonds in the aromatic

ring are found to be around an average value of 1.39 Å. As far as the bond angles are considered, the OCN bond angles O(3)-C(8)-N(6), O(1)-C(9)-N(4), O(2)-C(12)-N(4) and O(2)-C(12)-N(6) are found to be 120.377, 120.380, 123.081 and 123.089 ° respectively. The bond angle N(4)-C(12)-N(6) was observed to be 113.7968 °. The average C-C-C bond angle in the aromatic ring was 120 °. All these bond angles and bond distances are comparable with the values reported by Williams *et al* [23].

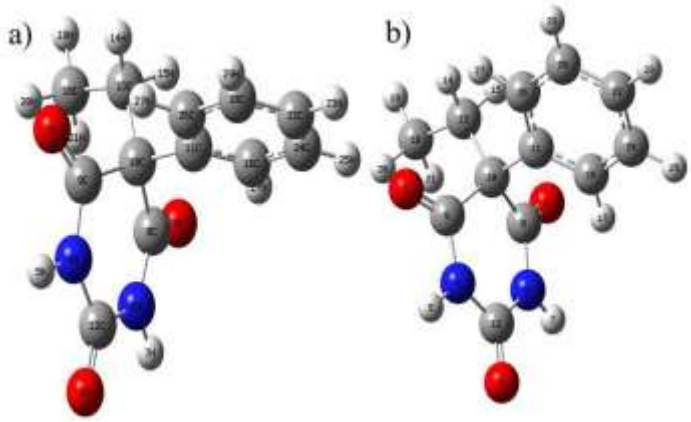

Figure 3. The geometry of phenobarbital molecule in gas phase (A) and in the active site of cytochrome P450 2B6 (B)

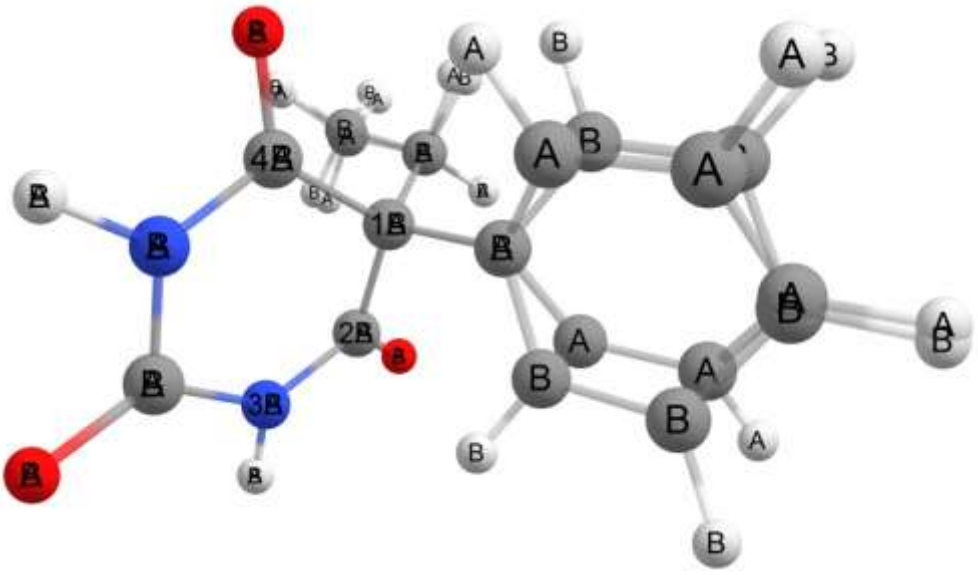

Figure 4. Structural overlay of phenobarbital molecule in gas phase (A) and in active site region (B).

Table 3. Bond lengths (Å), bond angles (°),Torsion angles (°) of phenobarbital molecule active site environment.

Bonds	DFT
Bond lengths (Å)	
O(1)-C(9)	1.2097
O(2)-C(12)	1.2061
O(3)-C(8)	1.2097
N(4)-H(5)	1.0124
N(4)-C(9)	1.3883
N(4)-C(12)	1.3892
N(6)-H(7)	1.0124
N(6)-C(8)	1.3884
N(6)-C(12)	1.3891
C(8)-C(10)	1.5363
C(9)-C(10)	1.5363
C(10)-C(11)	1.5587
C(10)-C(13)	1.5515
C(11)-C(16)	1.4003
C(11)-C(26)	1.4002
C(13)-H(14)	1.0911
C(13)-H(15)	1.0911
C(13)-C(18)	1.5313
C(16)-H(17)	1.0821
C(16)-C(24)	1.3928
C(18)-H(19)	1.0928
C(18)-H(20)	1.0924
C(18)-H(21)	1.0924
C(22)-H(23)	1.0839
C(22)-C(24)	1.3916
C(22)-C(28)	1.3916
C(24)-H(25)	1.0841
C(26)-H(27)	1.0821
C(26)-C(28)	1.3928
C(28)-H(29)	1.0841
Bond angles (˚)	
H(5)-N(4)-C(9)	116.5537
H(5)-N(4)-C(12)	115.3579
C(9)-N(4)-C(12)	127.613
H(7)-N(6)-C(8)	116.548
H(7)-N(6)-C(12)	115.3635

C(8)-N(6)-C(12)	127.6072
O(3)-C(8)-N(6)	120.377
O(3)-C(8)-C(10)	123.2673
N(6)-C(8)-C(10)	116.2639
O(1)-C(9)-N(4)	120.3804
O(1)-C(9)-C(10)	123.2603
N(4)-C(9)-C(10)	116.268
C(8)-C(10)-C(9)	111.8947
C(8)-C(10)-C(11)	107.7864
C(8)-C(10)-C(13)	110.0688
C(9)-C(10)-C(11)	107.7977
C(9)-C(10)-C(13)	110.068
C(11)-C(10)-C(13)	109.1356
C(10)-C(11)-C(16)	120.6891
C(10)-C(11)-C(26)	120.6987
C(16)-C(11)-C(26)	118.501
O(2)-C(12)-N(4)	123.0812
O(2)-C(12)-N(6)	123.0899
N(4)-C(12)-N(6)	113.7968
C(10)-C(13)-H(14)	106.8978
C(10)-C(13)-H(15)	106.8963
C(10)-C(13)-C(18)	115.1787
H(14)-C(13)-H(15)	107.5814
H(14)-C(13)-C(18)	109.9852
H(15)-C(13)-C(18)	109.9839
C(11)-C(16)-H(17)	120.2506
C(11)-C(16)-C(24)	120.6342
H(17)-C(16)-C(24)	119.1088
C(13)-C(18)-H(19)	109.6833
C(13)-C(18)-H(20)	111.6789
C(13)-C(18)-H(21)	111.6801
H(19)-C(18)-H(20)	107.3113
H(19)-C(18)-H(21)	107.3106
H(20)-C(18)-H(21)	108.9869
H(23)-C(22)-C(24)	120.3664
H(23)-C(22)-C(28)	120.3682
C(24)-C(22)-C(28)	119.2645
C(16)-C(24)-C(22)	120.4789
C(16)-C(24)-H(25)	119.3107
C(22)-C(24)-H(25)	120.2103
C(11)-C(26)-H(27)	120.2531

C(11)-C(26)-C(28)	120.6339
H(27)-C(26)-C(28)	119.1065
C(22)-C(28)-C(26)	120.479
C(22)-C(28)-H(29)	120.212
C(26)-C(28)-H(29)	119.309
Torsion angles (˚)	
H(5)-N(4)-C(9)-O(1)	-3.5559
H(5)-N(4)-C(9)-C(10)	173.0805
C(12)-N(4)-C(9)-O(1)	168.1103
C(12)-N(4)-C(9)-C(10)	-15.2533
H(5)-N(4)-C(12)-O(2)	-5.8218
H(5)-N(4)-C(12)-N(6)	172.171
C(9)-N(4)-C(12)-O(2)	-177.573
C(9)-N(4)-C(12)-N(6)	0.42
H(7)-N(6)-C(8)-O(3)	3.5707
H(7)-N(6)-C(8)-C(10)	-173.058
C(12)-N(6)-C(8)-O(3)	-168.045
C(12)-N(6)-C(8)-C(10)	15.3262
H(7)-N(6)-C(12)-O(2)	5.833
H(7)-N(6)-C(12)-N(4)	-172.16
C(8)-N(6)-C(12)-O(2)	177.533
C(8)-N(6)-C(12)-N(4)	-0.4596
O(3)-C(8)-C(10)-C(9)	155.9301
O(3)-C(8)-C(10)-C(11)	-85.7183
O(3)-C(8)-C(10)-C(13)	33.2099
N(6)-C(8)-C(10)-C(9)	-27.5482
N(6)-C(8)-C(10)-C(11)	90.8034
N(6)-C(8)-C(10)-C(13)	-150.268
O(1)-C(9)-C(10)-C(8)	-155.954
O(1)-C(9)-C(10)-C(11)	85.7011
O(1)-C(9)-C(10)-C(13)	-33.2333
N(4)-C(9)-C(10)-C(8)	27.5163
N(4)-C(9)-C(10)-C(11)	-90.8286
N(4)-C(9)-C(10)-C(13)	150.237
C(8)-C(10)-C(11)-C(16)	31.5351
C(8)-C(10)-C(11)-C(26)	-152.356
C(9)-C(10)-C(11)-C(16)	152.4851
C(9)-C(10)-C(11)-C(26)	-31.4062
C(13)-C(10)-C(11)-C(16)	-87.9871
C(13)-C(10)-C(11)-C(26)	88.1216
C(8)-C(10)-C(13)-H(14)	-175.598

C(8)-C(10)-C(13)-H(15)	-60.6241
C(8)-C(10)-C(13)-C(18)	61.8875
C(9)-C(10)-C(13)-H(14)	60.6134
C(9)-C(10)-C(13)-H(15)	175.5874
C(9)-C(10)-C(13)-C(18)	-61.901
C(11)-C(10)-C(13)-H(14)	-57.4989
C(11)-C(10)-C(13)-H(15)	57.475
C(11)-C(10)-C(13)-C(18)	179.9866
C(10)-C(11)-C(16)-H(17)	-1.9491
C(10)-C(11)-C(16)-C(24)	177.1193
C(26)-C(11)-C(16)-H(17)	-178.142
C(26)-C(11)-C(16)-C(24)	0.9265
C(10)-C(11)-C(26)-H(27)	1.9454
C(10)-C(11)-C(26)-C(28)	-177.121
C(16)-C(11)-C(26)-H(27)	178.1378
C(16)-C(11)-C(26)-C(28)	-0.9287
C(10)-C(13)-C(18)-H(19)	-179.992
C(10)-C(13)-C(18)-H(20)	61.1728
C(10)-C(13)-C(18)-H(21)	-61.1576
H(14)-C(13)-C(18)-H(19)	59.1618
H(14)-C(13)-C(18)-H(20)	-59.6731
H(14)-C(13)-C(18)-H(21)	177.9965
H(15)-C(13)-C(18)-H(19)	-59.1494
H(15)-C(13)-C(18)-H(20)	-177.984
H(15)-C(13)-C(18)-H(21)	59.6853
C(11)-C(16)-C(24)-C(22)	-0.2177
C(11)-C(16)-C(24)-H(25)	179.8995
H(17)-C(16)-C(24)-C(22)	178.8613
H(17)-C(16)-C(24)-H(25)	-1.0216
H(23)-C(22)-C(24)-C(16)	179.8298
H(23)-C(22)-C(24)-H(25)	-0.2884
C(28)-C(22)-C(24)-C(16)	-0.5043
C(28)-C(22)-C(24)-H(25)	179.3775
H(23)-C(22)-C(28)-C(26)	-179.832
H(23)-C(22)-C(28)-H(29)	0.287
C(24)-C(22)-C(28)-C(26)	0.5022
C(24)-C(22)-C(28)-H(29)	-179.379
C(11)-C(26)-C(28)-C(22)	0.222
C(11)-C(26)-C(28)-H(29)	-179.896
H(27)-C(26)-C(28)-C(22)	-178.855
H(27)-C(26)-C(28)-H(29)	1.0271

3.3. Topological analysis

In understanding the various bonding and non-bonding interactions between a ligand and a protein as well as the reactive nature of the ligand, it is important to analyze the charge density distribution and the electrostatic properties of ligand molecule and the neighboring amino acids of active site[24], [25]. Bader's quantum theory of atoms in molecules (QTAIM)[16], [26] was employed for the charge density analysis of phenobarbital molecule in both the forms. The electron density and Laplacian of electron density at the bond critical points (*bcp*) of all the bonds of the gas phase molecule and the one lifted from the active site are collected in Table 4. As it can be observed, there is no much difference in the values between the two forms.

The deformation of electron density maps of the two rings of the active site form of phenobarbital molecule have been plotted and shown in Figure 5. The maps show the charge accumulation areas of the molecule and allow one to visualize the lone pair positions of atoms in the molecule. The $\rho_{bcp}(r)$ values of the aromatic C-C bonds range from 1.557 eA^{-3} to 2.099 eA^{-3}. The $\rho_{bcp}(r)$ of the three C=O bonds were found to be 2.8 (C9-O1), 2.851 (C12-O2) and 2.8 (C8-O3) eA^{-3}. The two C–N bonds (C8-N6 and C9-N4) have an equal electron density of 2.032 eA^{-3}. Similarly, the $\rho_{bcp}(r)$ values of other two C–N bonds, C12-N4 and C12-N6 were found to be 2.067 eA^{-3}.

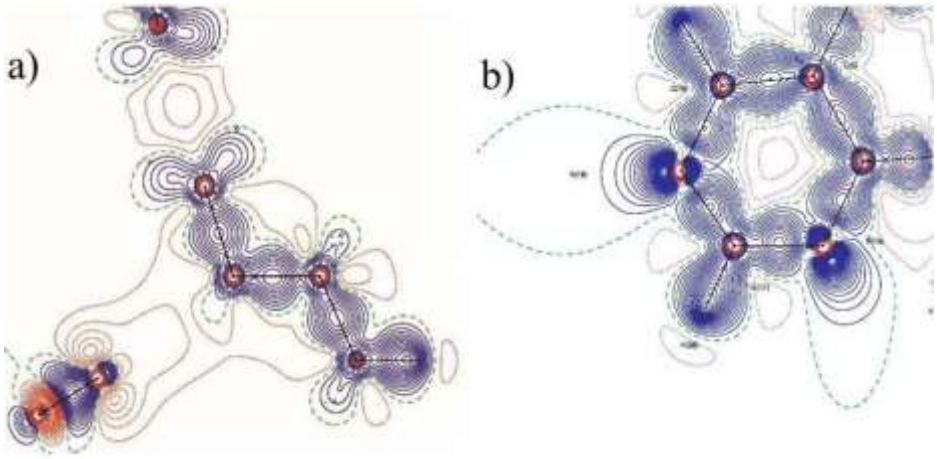

Figure 5. (a) – (b) showing the deformation density maps of phenobarbital molecule active site of cytochrome P450 2B6 receptor. Solid lines indicate positive contours, dotted lines are negative and dashed lines are zero contours. The contour interval is 0.05 $eÅ^{-3}$.

The Laplacian of electron density gives the important features about chemical bonding of molecules and whether the charges are concentrated or depleted at the bond critical point (*bcp*).

The Laplacian of electron density maps of the aromatic ring and pyrimidine ring have been plotted and shown in Figure 6. The Laplacian of electron density $\nabla^2\rho(r)$ of both forms of molecule has been calculated and no deviation was found between the forms Table.4. Figure 7. (a-b) of gasphase and active site $\nabla^2\rho(r)$ values of the aromatic C–C bonds range from -11.929 eA^{-5} to -21.089 eA^{-5}. The $\nabla^2\rho(r)$ of the three C=O bonds were found to be -4.5 (C9-O1), -7.28 (C12-O2) and -4.5 (C8-O3) eA^{-5}. The $\nabla^2\rho(r)$ of the four C–N bonds C8-N6, C9-N4, C12-N4 and C12-N6 were found to be -20.413 eA^{-5},-20.417 eA^{-5}, -21.906 eA^{-5} and -20.898 eA^{-5} respectively.

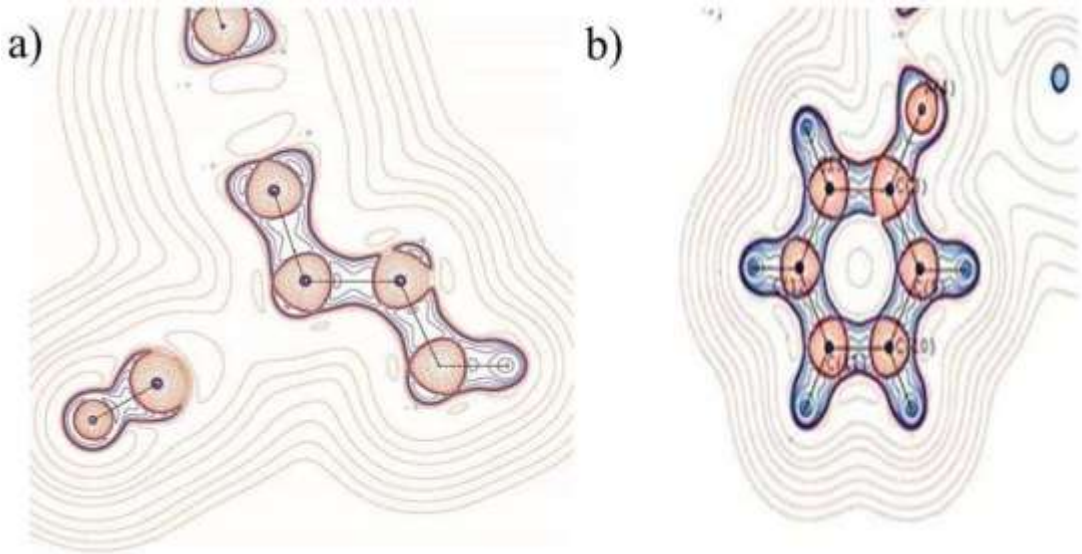

Figure 6. (a) – (b) showing the Laplacian of electron density maps of phenobarbital molecule active site of cytochrome P450 2B6 receptor. Contours are drawn in logarithmic scale, 3.0 x 2^N $eÅ^{-5}$.

Table 4. Electron density and Laplacian of electron density of gas phase and active site surrounding phenobarbital.

	Gas phase		Active site	
Bonds	$\rho_{bcp}(r)$	$\nabla^2\rangle(\rho)$	$\rho_{bcp}(r)$	$\nabla^2\rangle(\rho)$
C(9)-N(4)	2.032	-20.417	2.031	-20.407
N(4)-C(12)	2.067	-21.898	2.071	-21.974
H(5)-N(4)	2.276	-40.649	2.275	-40.68
C(12)-N(6)	2.067	-21.906	2.068	-21.907
C(8)-N(6)	2.032	-20.413	2.029	-20.297

C(12)-O(2)	2.851	-7.287	2.85	-7.346
N(6)-H(7)	2.276	-40.65	2.27	-40.39
C(9)-C(10)	1.662	-13.548	1.658	-13.484
C(10)-C(8)	1.662	-13.55	1.66	-13.514
C(8)-O(3)	2.8	-4.5	2.804	-4.495
O(1)-C(9)	2.8	-4.508	2.798	-4.1079
C(11)-C(10)	1.526	-11.219	1.528	-11.252
C(13)-C(10)	1.557	-11.768	1.564	-11.929
C(13)-C(18)	1.615	-12.873	1.615	-12.878
H(14)-C(13)	1.888	-22.725	1.793	-20.409
C(13)-H(15)	1.888	-22.725	1.792	-20.464
C(11)-C(16)	2.058	-19.992	2.062	-20.032
C(16)-H(17)	1.927	-23.86	1.84	-21.784
H(19)-C(18)	1.848	-21.823	1.766	-20.134
H(20)-C(18)	1.856	-21.979	1.773	-20.009
C(18)-H(21)	1.856	-21.979	1.769	-19.93
C(24)-C(16)	2.089	-20.815	2.09	-20.846
C(22)-C(24)	2.099	-21.072	2.101	-21.095
C(28)-C(22)	2.099	-21.073	2.099	-21.089
H(23)-C(22)	1.906	-23.444	1.832	-21.748
C(24)-H(25)	1.906	-23.444	1.833	-21.76
C(26)-C(11)	2.058	-19.994	2.053	-19.908
C(28)-C(26)	2.089	-20.813	2.091	-20.825
H(27)-C(26)	1.927	-23.86	1.84	-21.843
H(29)-C(28)	1.906	-23.443	1.834	-21.78

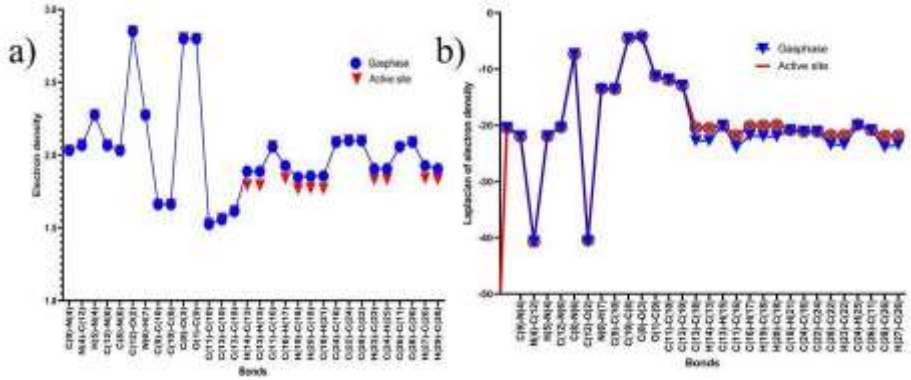

Figure 7. The difference of electron density and Laplacian of electron density distribution (a-b) of gasphase and active site of phenobarbital.

3.4. Atomic charges and Dipole moment

The atomic charges for the PB molecule in both the surroundings were calculated from Mulliken population analysis (MPA)[27], natural population analysis (NPA)[28] and Bader's AIM analysis[29] and the results are presented in Table 5. Strong and weak intermolecular interactions between the ligand and receptor in the active site have led to a change in the conformation of the PB molecule, leading to charge redistribution. The carbon atoms C8, C9 and C12 bound to oxygen atoms O3, O1 and O2 respectively carry high positive charge as anticipated, which may be due to the electron polarization towards the more electronegative oxygen atom. Owing to the intermolecular interactions between the amino acids of the receptor and the oxygen atoms of the ligand, the MPA charges of the oxygen atoms are found to be slightly less negative compared to that of the gas phase.

Table 5. Atomic charges(e) of phenobarbital gas form and in active site form.

	Gas phase			Active site		
Atoms	MPA	NPA	AIM	MPA	NPA	AIM
O(1)	-0.321	-0.586	-1.12	-0.318	-0.576	-1.12
O(2)	-0.324	-0.586	-1.12	-0.324	-0.587	-1.12
O(3)	-0.321	-0.586	-1.12	-0.301	-0.567	-1.12
N(4)	-0.426	-0.658	-1.13	-0.427	-0.659	-1.13
H(5)	0.256	0.423	0.43	0.257	0.424	0.43
N(6)	-0.426	-0.658	-1.13	-0.412	-0.666	-1.13
H(7)	0.256	0.423	0.43	0.257	0.424	0.43
C(8)	0.461	0.729	1.38	0.406	0.72	1.38
C(9)	0.461	0.729	1.38	0.496	0.726	1.38
C(10)	-0.398	-0.228	0	-0.427	-0.233	0
C(11)	-0.082	-0.015	-0.04	-0.018	-0.011	-0.04
C(12)	0.5	0.836	1.8	0.497	0.835	1.8
C(13)	-0.123	-0.358	0.06	-0.131	-0.372	0.06
H(14)	0.135	0.215	0.02	0.124	0.212	0.02

H(15)	0.135	0.215	0.02	0.137	0.225	0.02
C(16)	-0.048	-0.209	-0.02	-0.054	-0.207	-0.02
H(17)	0.117	0.221	0.05	0.1	0.209	0.05
C(18)	-0.304	-0.576	0.02	-0.311	-0.579	0.02
H(19)	0.115	0.206	0	0.119	0.214	0
H(20)	0.115	0.197	0	0.117	0.2	0
H(21)	0.115	0.197	0	0.11	0.193	0
C(22)	-0.076	-0.193	-0.01	-0.075	-0.194	-0.01
H(23)	0.099	0.204	0.02	0.099	0.208	0.02
C(24)	-0.092	-0.183	-0.01	-0.096	-0.187	-0.01
H(25)	0.1	0.204	0.02	0.1	0.208	0.02
C(26)	-0.048	-0.209	-0.02	-0.041	-0.199	-0.02
H(27)	0.117	0.221	0.05	0.11	0.218	0.05
C(28)	-0.092	-0.183	-0.01	-0.094	-0.188	-0.01
H(29)	0.1	0.204	0.02	0.1	0.208	0.02

The dipole moments were calculated for the PB molecule in gas phase and for the one lifted from the active site (Table 6). The dipole moment value of the PB in gas phase is 1.4397 D, whereas the corresponding active site value is 1.5898 D. This considerable difference between the dipole moment values of PB in the gas phase and active site supports the interaction of PB with CYP2B6 enzyme. This dipole difference between the two forms corroborates the operation of hydrogen bonding, alkyl, π-alkyl, and Pi-cation interactions between PB and the amino acid residues of CYP2B6 enzyme. Figure 8, shows the orientation of dipole moment vectors of gas phase and active site PB molecule.

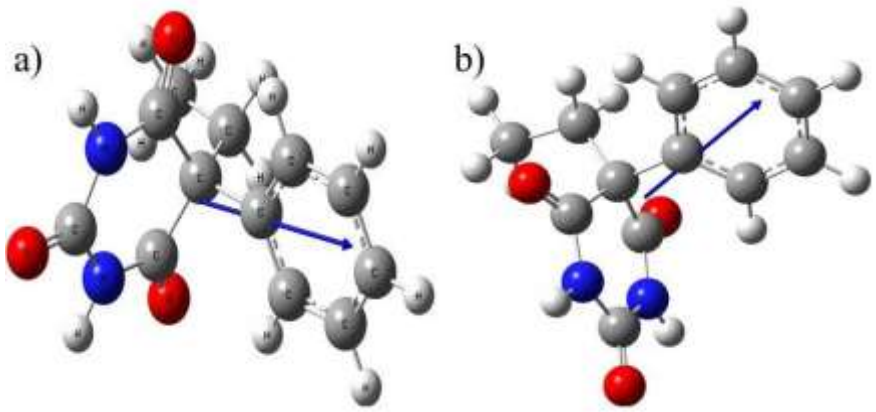

Figure 8. Molecular dipole moment vectors of forms gas phase (A) and the active site (B) of PB showing the orientational difference in different phases. The origin is at the center of mass of the molecule.

Table 6. Dipole moments (Debye) of PB molecule in gas phase and in the active site of cytochrome P450 2B6

Dipole	Gas Phase	Active site
μ_x	1.4376	-1.5800
μ_y	-0.0773	-0.1671
μ_z	-0.0011	-0.0553
M	1.4397	1.5898

4.Conclusions

The present theoretical investigation analyzed the interaction between the potent anti-epileptic drug, phenobarbital and the human CYP2B6 enzyme, a monooxygenase system primarily expressed in the liver. The docking study revealed that the interaction between the H atom attached to N4 of the pyrimidine ring (ligand) and OE2 of GLU254 (protein) was the major contribution among all other type of interactions. The topological analysis in terms of electron density and Laplacian of electron density shows that there is only a minimum deviation in the values between the gas phase and the one lifted from the active site. The studies on atomic charges and electrostatic potential maps of two different forms of phenobarbital confirm the charge redistribution and

formation of electronegative and electropositive regions in the inhibitor molecule. The greater dipole moment of the gas phase form of the phenobarbital molecule in comparison with the active site form indicates the interaction between the inhibitor and the enzyme.

References

[1] *W. H. Organization, "Epilepsy: a public health imperative: summary," World Health Organization, 2019.*

[2] *A. C. Swann, "Major system toxicities and side effects of anticonvulsants," J. Clin. Psychiatry, vol. 62, no. Suppl 14, pp. 16–21, 2001.*

[3] *L. Gervot et al., "Human CYP2B6: expression, inducibility and catalytic activities," Pharmacogenet. Genomics, vol. 9, no. 3, pp. 295–306, 1999.*

[4] *D. M. Stresser and D. Kupfer, "Monospecific antipeptide antibody to cytochrome P-450 2B6," Drug Metab. Dispos., vol. 27, no. 4, pp. 517–525, 1999.*

[5] *A. Rostami-Hodjegan and G. T. Tucker, "Simulation and prediction of in vivo drug metabolism in human populations from in vitro data," Nat. Rev. Drug Discov., vol. 6, no. 2, pp. 140–148, 2007.*

[6] *D. M. Feidt et al., "Profiling induction of cytochrome p450 enzyme activity by statins using a new liquid chromatography-tandem mass spectrometry cocktail assay in human hepatocytes," Drug Metab. Dispos., vol. 38, no. 9, pp. 1589–1597, 2010.*

[7] *T. Sueyoshi, T. Kawamoto, I. Zelko, P. Honkakoski, and M. Negishi, "The repressed nuclear receptor CAR responds to phenobarbital in activating the human CYP2B6 gene," J. Biol. Chem., vol. 274, no. 10, pp. 6043–6046, 1999.*

[8] *S. R. Faucette et al., "Relative activation of human pregnane X receptor versus constitutive androstane receptor defines distinct classes of CYP2B6 and CYP3A4 inducers," J. Pharmacol. Exp. Ther., vol. 320, no. 1, pp. 72–80, 2007.*

[9] *O. Pelkonen, M. Turpeinen, J. Hakkola, P. Honkakoski, J. Hukkanen, and H. Raunio, "Inhibition and induction of human cytochrome P450 enzymes: current status," Arch. Toxicol., vol. 82, no. 10, pp. 667–715, 2008.*

[10] H. Remmer and H. J. Merker, "Drug-induced changes in the liver endoplasmic reticulum: association with drug-metabolizing enzymes," Science (80-.)., vol. 142, no. 3600, pp. 1657–1658, 1963.

[11] T. Saussele et al., "Selective induction of human hepatic cytochromes P450 2B6 and 3A4 by metamizole," Clin. Pharmacol. Ther., vol. 82, no. 3, pp. 265–274, 2007.

[12] O. A. Fahmi et al., "Evaluation of CYP2B6 induction and prediction of clinical drug–drug interactions: considerations from the IQ consortium induction working group—an industry perspective," Drug Metab. Dispos., vol. 44, no. 10, pp. 1720–1730, 2016.

[13] G. M. Morris, "D: S: Goodsell, RS Halliday, R. Huey, WE Hart, RK Belew," AJ Olson, J. Comput. Chem, vol. 19, pp. 1639–1662, 1998.

[14] M. Frisch et al., "gaussian 09, Revision d. 01, Gaussian," Inc., Wallingford CT, vol. 201, 2009.

[15] S. J. Smith and B. T. Sutcliffe, "The development of computational chemistry in the United Kingdom," Rev. Comput. Chem., pp. 271–316, 1996.

[16] R. F. W. Bader, Y. Tal, S. G. Anderson, and T. T. Nguyen-Dang, "Quantum topology: theory of molecular structure and its change," Isr. J. Chem., vol. 19, no. 1-4, pp. 8–29, 1980.

[17] R. F. W. Bader, "International Series of Monographs on Chemistry," Atoms Mol. A Quantum Theory, vol. 22, 1990.

[18] J. Cheeseman, T. A. Keith, and R. F. W. Bader, "AIMPAC program package," McMaster Univ. Hamilton, Ontario, vol. 18, 1992.

[19] T. A. Keith, "AIMAll, Version 09.02. 01," Available aim@ tkgristmill. com, 2009.

[20] T. Koritsanszky et al., "XD-2006," A Comput. Progr. Packag. multipole refinement Topol. Anal. Charg. densities Eval. Intermol. energies from Exp. or Theor. Struct. factors, Version, vol. 5, p. 33, 2007.

[21] T. S. Koritsanszky et al., "XD (version 4.10, July), a computer program package for multipole refinement and analysis of electron densities from diffraction data," Free Univ.

Berlin, Ger., 2003.

[22] C. B. Hübschle and P. Luger, "MolIso–a program for colour-mapped iso-surfaces," J. Appl. Crystallogr., vol. 39, no. 6, pp. 901–904, 2006.

[23] P. P. Williams, "Polymorphism of phenobarbitone: the crystal structure of 5-ethyl-5-phenylbarbituric acid monohydrate," Acta Crystallogr. Sect. B Struct. Crystallogr. Cryst. Chem., vol. 29, no. 8, pp. 1572–1579, 1973.

[24] C. Gatti and P. Macchi, "A Guided Tour Through Modern Charge Density Analysis," in Modern Charge-Density Analysis, Springer, 2011, pp. 1–78.

[25] R. F. W. Bader, "Atoms in molecules. International series of monographs in chemistry," 1994.

[26] C. F. Matta and R. J. Boyd, "An introduction to the quantum theory of atoms in molecules," Quantum Theory Atoms Mol. From Solid State to DNA Drug Des., 2007.

[27] R. Carbó-Dorca and P. Bultinck, "Quantum mechanical basis for Mulliken population analysis," J. Math. Chem., vol. 36, no. 3, pp. 231–239, 2004.

[28] A. E. Reed, R. B. Weinstock, and F. Weinhold, "Natural population analysis," J. Chem. Phys., vol. 83, no. 2, pp. 735–746, 1985.

[29] I. P. Grant, "Relativistic Quantum Theory of Atoms and Molecules, Volume 40 of Springer Series on Atomic, Optical, and Plasma Physics." Springer, New York, NY, 2007.